Stress and Electric Potential Fields in Piezoelectric Smart Spheres

A. Ghorbanpour*, S. Golabi, M. Saadatfar
Department of Mechanical Engineering University of Kashan, Kashan, Iran

Piezoelectric materials produce an electric field by deformation, and deform when subjected to an electric field. The coupling nature of piezoelectric materials has acquired wide applications in electric-mechanical and electric devices, including electric-mechanical actuators, sensors and structures. In this paper, a hollow sphere composed of a radially polarized spherically anisotropic piezoelectric material, e.g., PZT_5 or (Pb) (CoW) TiO_3 under internal or external uniform pressure and a constant potential difference between its inner and outer surfaces or combination of these loadings has been studied. Electrodes attached to the inner and outer surfaces of the sphere induce the potential difference. The governing equilibrium equations in radially polarized form are shown to reduce to a coupled system of second-order ordinary differential equations for the radial displacement and electric potential field. These differential equations are solved analytically for seven different sets of boundary conditions. The stress and the electric potential distributions in the sphere are discussed in detail for two piezoceramics, namely PZT_5 and (Pb) (CoW) TiO_3. It is shown that the hoop stresses in hollow sphere composed of these materials can be made virtually uniform across the thickness of the sphere by applying an appropriate set of boundary conditions.

Key Words: Smart Materials, Piezoelectric Hollow Sphere, Radial Stress, Hoop Stress, Electric Potential

1. Introduction

In recent years there has been a resurgence of interest in piezoelectricity, motivated by advances in smart structures technology. It is well known that piezoelectric materials produce an electric field when deformed, and undergo deformation when subjected to an electric field. The coupling nature of piezoelectric materials has attracted wide applications in electric-mechanical and electric devices, such as electric-mechanical actuators, sensors and transducers. For example, piezoelectric actuators can be used to modify the shape of an airfoil, thereby reducing transverse vortices (Destuynder, 1999), or to maintain proper tension with overhead electrical wires on a locomotive pantograph (Jiang et al., 1999). In addition to being used as actuators, which respond to changes in an electric field by producing mechanical strain, they can also be used as sensors, which respond to a mechanical strain by producing an electrical signal. One notable civil engineering application of piezoelectric sensors is in structural health monitoring (Kawiecki, 1999). A change in the level of strain will produce an electric charge and trigger sensors in the structure. The development of distributed piezoelectric sensors and actuators is essential for the design of future light-weight and high-performance structures with adaptive capabilities. In addition, various piezoelectric materials have been used in

* Corresponding Author,
E-mail : aghorban@kashanu.ac.ir
TEL : +98-0361-5570065; **FAX** : +98-0361-5559930
Department of Mechanical Engineering University of Kashan, Kashan, Iran. (Manuscript **Received** April 19, 2006; **Revised** August 17, 2006)

many transducer designs, sonar applications, medical ultrasonic equipment, robot tactile sensors, acoustic pick-ups, force and strain gages, etc. The advance in piezoelectric materials technology has a significant impact in diverse fields, such as the space and aircraft industries.

Piezoelectric materials show linearity between components of stress and strain, as well as between electric field and electric displacements, only over limited ranges of mechanical or electrical applied fields. The limits of linear behavior depend on the coercive field used to polarize the material and on material composition.

Because of the difficulty related to the particular coupling effect between electric field and mechanical deformation, few problems were considered before 1990. Spherical isotropy is a special kind of transverse isotropy that was introduced in 1865 by Saint-Venant, who gave an exact solution of a spherically isotropic spherical shell subjected to both internal and external uniform pressures (Love, 1927; Lekhnitskii, 1981).

Problems of radially-polarized piezoelectric bodies were considered and solved analytically (Chen, 1998). In the literature (Chen, 1998) the solution for isotropic medium provided static behavior such as stress concentration. Sinha (1962) obtained the solution of the problem of static radial deformation of a piezoelectric spherical shell and under a given voltage difference between these surfaces, coupled with a radial distribution of temperature from the inner to the outer surface.

New applications of a piezoelectric sensors and actuators are being introduced and expanded for a number of geometric configurations. In this paper, a hollow sphere composed of a radially polarized anisotropic piezoelectric material, e.g., PZT_5 or (Pb) (CoW) TiO_3, subjected to internal or external pressure and a constant potential difference between its inner and outer surfaces or combination of these loadings has been studied.

A brief summary of the constitutive equations for linear piezoelectric solids and also axisymmetric problem is formulated in the following section. The governing equilibrium equations in radially polarized form are reduced to a coupled system of second — order ordinary differential equations and are solved analytically for seven different sets of boundary conditions. Finally, stress and electric potential distributions are discussed in detail for two different piezoceramics, namely PZT_5 and (Pb) (CoW) TiO_3.

2. Basic Constitutive Equations

The governing constitutive equations for a homogeneous anisotropic piezoelectric solid can be written as (Berlincourt, 1971; Tiersten, 1969):

$$\varepsilon_{ij}=s_{ijkl}\sigma_{ij}+d_{mi}E_m \quad (i,j=1,\cdots,6) \tag{1}$$

$$D_m=e_{mi}\sigma_{ij}+\epsilon_{mk}{}^{\tau}E_k \quad (m,k=1,\cdots,3) \tag{2}$$

Where ε_{ij} and σ_{ij} are mechanical strains and s_{ijkl} stresses respectively, are elastic compliances, D_m are the components of electric displacement (also referred to as charge density), E_m are the components of electric field, d_{mi} are the piezoelectric module, in units of Columbs/Newton (C/N), which relate the electrical and mechanical effects and ϵ_{mk}^{T} are the dielectric permittivity constant at constant stress, in units Farads/Meter (F/M). An alternate, inverted form of the governing equations is (Berlincourt, 1971):

$$\sigma_{ij}=C_{ijkl}\varepsilon_{kl}-e_{mij}E_m \tag{3}$$

$$D_m=e_{mij}\varepsilon_{ij}+\epsilon_{mk}^{S}E_k \tag{4}$$

d_{mi} is replaced by e_{mij}, which represents the third order tensor of piezoelectric coefficient whose units are C/m^2, and the elastic compliances s_{ijkl} is replaced by elastic constants $c_{ijkl}\cdot\epsilon_{mk}$. denote the dielectric permittivity constants at constant strain (the superscript S has been dropped), in units of Farads/Meter (F/M). The notation can be contracted in standard fashion by noting that a single subscript for the stress components can represent the double subscript notation, e.g., $11=1, 22=2, 33=3, 23=4, 13=5$ and $12=6$. In final form, the rotated elastic stiffnesses are given by C_{11}, C_{22}, C_{33}, C_{44}, C_{55}, C_{66}, C_{12}, C_{13} and C_{23}. The non-zero elastic coefficients are represented by e_{11}, e_{12}, e_{13}, e_{26} and e_{35}, and non-zero dielectric constants by $\epsilon_{11}, \epsilon_{22}$ and ϵ_{33}. It is also noted that the electric field E_m can be written in terms of

electric potential ϕ as:

$$E=-\nabla\phi \tag{5}$$

In this study, two different piezoelectric materials were considered, i.e. PZT_5 and (Pb) (CoW) TiO_3, which are widely used in smart materials and structures technology.

3. Static Problem for a Hollow Sphere

A hollow sphere, with inner and outer radius of a and b respectively, subjected to axisymmetric mechanical and electrical loadings was considered in here (Fig. 1). The center of the spherical coordinate system (r, ζ, ϕ) considered in this research is located at the center of the hollow sphere. It is noted that when piezoelectric materials are poled spherically in the radial direction, they will exhibit spherical isotropy. The equilibrium equations, in the absence of body and inertia forces are (Fung, 1965):

$$\begin{aligned}
&\frac{\partial\sigma_{rr}}{\partial r}+\frac{1}{r\sin\zeta}\frac{\partial\sigma_{r\zeta}}{\partial\theta}+\frac{1}{r}\frac{\partial\sigma_{r\zeta}}{\partial\zeta}\\
&\quad+\frac{2\sigma_{rr}-\sigma_{\theta\theta}-\sigma_{\zeta\zeta}+\sigma_{r\zeta}\cot\zeta}{r}=0\\
&\frac{\partial\sigma_{r\zeta}}{r\partial}+\frac{1}{r\sin\zeta}\frac{\partial\sigma_{\theta\zeta}}{\partial\theta}+\frac{1}{r}\frac{\partial\sigma_{\zeta\zeta}}{\partial\zeta}\\
&\quad+\frac{3\sigma_{r\zeta}+(\sigma_{\zeta\zeta}-\sigma_{\theta\theta})\cot\zeta}{r}=0\\
&\frac{\partial\sigma_{r\theta}}{\partial r}+\frac{1}{r\sin\zeta}\frac{\partial\sigma_{\theta\theta}}{\partial\theta}+\frac{1}{r}\frac{\partial\sigma_{\theta\zeta}}{\partial\zeta}\\
&\quad+\frac{3\sigma_{r\theta}+2\sigma_{\theta\zeta}\cot\zeta}{r}=0
\end{aligned} \tag{6}$$

where σ_{ij} are the stress tensors.

In the absence of volume electric charges, the charge equation of electrostatics is given by Tiersten (1969):

$$\begin{aligned}
&\frac{\partial D_{rr}}{\partial r}+\frac{1}{r}\frac{\partial D_{\zeta}}{\partial\zeta}+\frac{2D_r}{r}\\
&+\frac{1}{r\sin\zeta}\frac{\partial D_{\theta}}{\partial\theta}+\frac{\cot\zeta}{r}D_{\zeta}=0
\end{aligned} \tag{7}$$

where D_r, D_θ and D_ζ are electric displacement components in the radial, circumferential and azimuthal directions, respectively.

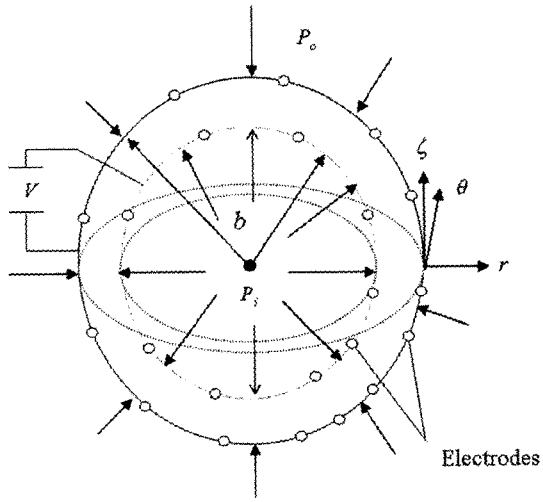

Fig. 1 Hollow sphere subject to uniform internal pressure P_i, uniform external pressure P_o and applied voltage V

The strain-displacement relations can be written in the spherical coordinate system as:

$$\begin{aligned}
\varepsilon_{rr}&=\frac{\partial u}{\partial r}\\
\varepsilon_{\zeta\zeta}&=\frac{1}{r}\frac{\partial v}{\partial\zeta}+\frac{u}{r}\\
\varepsilon_{\theta\theta}&=\frac{1}{r\sin\zeta}\frac{\partial w}{\partial\theta}+\frac{\cot\zeta}{r}v+\frac{u}{r}\\
\varepsilon_{r\zeta}&=\frac{1}{r}\frac{\partial u}{\partial\zeta}+\frac{\partial v}{\partial r}-\frac{v}{r}\\
\varepsilon_{\zeta\theta}&=\frac{1}{r\sin\zeta}\frac{\partial v}{\partial\theta}+\frac{1}{r}\frac{\partial w}{\partial\zeta}-\frac{\cot\zeta}{r}w\\
\varepsilon_{r\theta}&=\frac{1}{r\sin\zeta}\frac{\partial u}{\partial\theta}+\frac{\partial w}{\partial r}-\frac{w}{r}
\end{aligned} \tag{8}$$

where $\varepsilon_{rr}, \varepsilon_{\theta\theta}$ and $\varepsilon_{\zeta\zeta}$ are the components of the linear strain tensor, and $\varepsilon_{r\zeta}, \varepsilon_{\zeta\theta}$ and $\varepsilon_{r\theta}$ are the components of engineering shear strain. The displacement components are defined in radial μ, azimuthal v, and circumferential w directions. The electric field components E_i are related potential $\phi(r, \zeta, \theta)$ using the relations:

$$\begin{aligned}
E_{rr}&=-\frac{\partial\phi}{\partial r}\\
E_{\zeta\zeta}&=-\frac{1}{r}\frac{\partial\phi}{\partial\zeta}\\
\varepsilon_{\theta\theta}&=-\frac{1}{r\sin\zeta}\frac{\partial\phi}{\partial\theta}
\end{aligned} \tag{9}$$

In this paper, an analytic solution to the axisymmetric problem, radially polarized, radially orthotropic piezoelectric hollow sphere were developed. The displacement field is assumed as:

$$\begin{aligned} U_r &= u(r) \\ U_\xi &= 0 \\ U_\theta &= 0 \\ \phi &= \phi(r) \end{aligned} \tag{10}$$

Substituting these displacement functions into equation (8), strain displacement relations can be written as:

$$\begin{aligned} \varepsilon_{rr} &= \frac{\partial u}{\partial r} \\ \varepsilon_{\xi\xi} &= \frac{u}{r} \\ \varepsilon_{\theta\theta} &= \frac{u}{r} \\ E_r &= -\frac{\partial \phi}{\partial r} \end{aligned} \tag{11}$$

The constitutive relations of spherically isotropic radially polarized piezoelectric media also read as (Sinha, 1962; Chen and Shioya, 2001):

$$\begin{aligned} \sigma_{rr} &= C_{11}\varepsilon_{rr} + C_{12}\varepsilon_{\theta\theta} + C_{13}\varepsilon_{\xi\xi} - e_{11}E_r \\ \sigma_{\theta\theta} &= C_{12}\varepsilon_{rr} + C_{22}\varepsilon_{\theta\theta} + C_{23}\varepsilon_{\xi\xi} - e_{12}E_r \\ \sigma_{\xi\xi} &= C_{13}\varepsilon_{rr} + C_{23}\varepsilon_{\theta\theta} + C_{33}\varepsilon_{\xi\xi} - e_{12}E_r \end{aligned} \tag{12}$$

Substitution of equations (9) and (11) in (12), leads to:

$$\begin{aligned} \sigma_{rr} &= C_{11}\frac{\partial u}{\partial r} + (C_{12}+C_{13})\frac{u}{r} + e_{11}\frac{d\phi}{dr} \\ \sigma_{\theta\theta} &= C_{12}\frac{\partial u}{\partial r} + (C_{22}+C_{23})\frac{u}{r} + e_{12}\frac{d\phi}{dr} \\ \sigma_{\xi\xi} &= C_{13}\frac{\partial u}{\partial r} + (C_{23}+C_{33})\frac{u}{r} + e_{12}\frac{d\phi}{dr} \end{aligned} \tag{13}$$

Substituting displacement functions (11), into stress-strain relations (12), the field-potential relations (9), the equations of equilibrium (6), and the charge equation of electrostatics (7) yield the following two equations:

$$\begin{aligned} &C_{11}\frac{\partial^2 u}{\partial r^2} + 2\frac{C_{11}}{r}\frac{\partial u}{\partial r} + \frac{2}{r^2}(C_{12}-C_{23}-C_{22})u \\ &\quad + e_{21}\frac{\partial^2 \phi}{\partial r^2} + \frac{2}{r}(e_{11}-e_{12})\frac{\partial \phi}{\partial r} = 0 \\ &e_{11}\frac{\partial^2 u}{\partial r^2} + \frac{2}{r}(e_{11}+e_{12})\frac{\partial u}{\partial r} + \frac{2}{r^2}e_{12}u \\ &\quad - \epsilon_{11}\frac{\partial^2 \phi}{\partial r^2} - \frac{2\epsilon_{12}}{r}\frac{\partial \phi}{\partial r} = 0 \end{aligned} \tag{14}$$

Equations (14) constitute a coupled system of linear second-order ordinary differential equations for $u(r)$ and ϕr. In absence of free charge density, the charge equation in the case where there is radial symmetry can be rewritten as:

$$\frac{\partial D_r}{\partial r} + \frac{2}{r}D_r = 0 \tag{15}$$

where D_r is the component of radial electric displacement. The solution to this equation is:

$$D_r = \frac{A_1}{r^2} \tag{16}$$

where A_1 is a constant. Substituting the displacement functions into the piezoelectric constitutive equation and reducing the equation of equilibrium and the charge equation to a single equation results:

$$\begin{aligned} &\left(C_{11}+\frac{e_{11}^2}{\epsilon_{11}}\right)\frac{\partial^2 u}{\partial r^2} + \frac{2}{r}\left(C_{11}+\frac{e_{11}^2}{\epsilon_{11}}\right)\frac{\partial u}{\partial r} \\ &+ \frac{2}{r^2}\left[C_{12}-C_{23}-C_{22}+\frac{e_{12}}{\epsilon_{11}}(e_{11}-2e_{12})\right]u = -\frac{2A_1e_{12}}{\epsilon_{11}r^3} \end{aligned} \tag{17}$$

Accordingly equation (17) can be written to the simpler form of:

$$\frac{\partial^2 u}{\partial r^2} + \frac{2}{r}\frac{\partial u}{\partial r} - \frac{2}{r^2}\beta u = -\frac{2A_1e_{12}}{\epsilon_{11}\gamma r^3} \tag{18}$$

where

$$\beta = \frac{C_{22}+C_{23}-C_{12}+\dfrac{e_{12}}{\epsilon_{12}}(2e_{12}-e_{11})}{C_{11}+\dfrac{e_{11}^2}{\epsilon_{11}}} \tag{19}$$

and

$$\gamma = C_{11}+\frac{e_{11}^2}{\epsilon_{11}} \tag{20}$$

The solution to equation (18) for $u(r)$ can be written as:

$$u(r) = F_1\gamma^{a_1} + F_2r^{a_2} + \frac{A_1e_{12}}{\beta\epsilon_{11}\gamma r} \tag{21}$$

where F_1, F_2 and A_1 are constants, and

$$\alpha_{1,2}=\frac{-1\pm\sqrt{1+8\beta}}{2} \tag{22}$$

Integrating the expression for $\phi(r)$ yields:

$$\phi(r)=\frac{e_{11}}{\epsilon_{11}}u+2\frac{e_{12}}{\epsilon_{11}}\int\frac{u}{r}dr+\frac{A_1}{\epsilon_{11}r}+A_2 \tag{23}$$

where A_2 is a constant. Since $u(r)$ is known, the electrostatic potential is computed as:

$$\begin{aligned}\phi(r)=&\left(\frac{e_{11}}{\epsilon_{11}}+\frac{2}{\alpha_1}\frac{e_{12}}{\epsilon_{11}}\right)F_1r^{\alpha_1}+\left(\frac{e_{11}}{\epsilon_{11}}+\frac{2}{\alpha_2}\frac{e_{12}}{\epsilon_{11}}\right)F_2r^{\alpha_2}\\&+\frac{A_1}{r}\left(-\frac{2e_{12}}{\epsilon_{11}}\frac{e_{12}}{\beta\gamma\epsilon_{11}}+\frac{e_{11}}{\epsilon_{11}}\frac{e_{12}}{\beta\epsilon_{11}}\gamma+\frac{1}{\epsilon_{11}}\right)+A_2\end{aligned} \tag{24}$$

Substituting the expressions for $u(r)$ and from (21) and (24) into (13), results:

$$\begin{aligned}\sigma_{rr}=&F_1\left(C_{11}\alpha_1+2C_{12}+\alpha_1e_{11}\left(\frac{e_{11}}{\epsilon_{11}}+\frac{2}{\alpha_1}\frac{e_{12}}{\epsilon_{11}}\right)\right)r^{(\alpha_1-1)}\\&+F_2\left(C_{11}\alpha_2+2C_{12}+\alpha_2e_{11}\left(\frac{e_{11}}{\epsilon_{11}}+\frac{2}{\alpha_2}\frac{e_{12}}{\epsilon_{11}}\right)\right)r^{(\alpha_2-1)}\\&+A_1\left[\frac{1}{r^2}\left((2C_{12}-C_{11})\frac{e_{12}}{\beta\gamma\epsilon_{11}}\right.\right.\\&\left.\left.-e_{11}\left(-\frac{2e_{12}}{\epsilon_{11}}\frac{e_{12}}{\beta\gamma\epsilon_{11}}+\frac{e_{11}}{\epsilon_{11}}\frac{e_{12}}{\beta\epsilon_{11}}\gamma+\frac{1}{\epsilon_{11}}\right)\right)\right]\end{aligned} \tag{25}$$

$$\begin{aligned}\sigma_{\theta\theta}=&F_1\left(C_{12}\alpha_1+(C_{22}+C_{23})+\alpha_1e_{12}\left(\frac{e_{11}}{\epsilon_{11}}+\frac{2}{\alpha_1}\frac{e_{12}}{\epsilon_{11}}\right)\right)r^{(\alpha_1-1)}\\&+F_2\left(C_{12}\alpha_2+(C_{22}+C_{23})+\alpha_2e_{12}\left(\frac{e_{11}}{\epsilon_{11}}+\frac{2}{\alpha_2}\frac{e_{12}}{\epsilon_{11}}\right)\right)r^{(\alpha_2-1)}\\&+A_1\left[\frac{1}{r^2}\left((C_{22}+C_{23}-C_{12})\frac{e_{12}}{\beta\gamma\epsilon_{11}}\right.\right.\\&\left.\left.-e_{12}\left(-\frac{2e_{12}}{\epsilon_{11}}\frac{e_{12}}{\beta\gamma\epsilon_{11}}+\frac{e_{11}}{\epsilon_{11}}\frac{e_{12}}{\beta\epsilon_{11}}\gamma+\frac{1}{\epsilon_{11}}\right)\right)\right]\end{aligned} \tag{26}$$

$$\begin{aligned}\sigma_{zz}=&F_1\left(C_{13}\alpha_1+(C_{23}+C_{33})+\alpha_1e_{12}\left(\frac{e_{11}}{\epsilon_{11}}+\frac{2}{\alpha_1}\frac{e_{12}}{\epsilon_{11}}\right)\right)r^{(\alpha_1-1)}\\&+F_2\left(C_{13}\alpha_2+(C_{23}+C_{33})+\alpha_2e_{12}\left(\frac{e_{11}}{\epsilon_{11}}+\frac{2}{\alpha_2}\frac{e_{12}}{\epsilon_{11}}\right)\right)r^{(\alpha_2-1)}\\&+A_1\left[\frac{1}{r^2}\left((C_{23}+C_{33}-C_{13})\frac{e_{12}}{\beta\gamma\epsilon_{11}}\right.\right.\\&\left.\left.-e_{12}\left(-\frac{2e_{12}}{\epsilon_{11}}\frac{e_{12}}{\beta\gamma\epsilon_{11}}+\frac{e_{11}}{\epsilon_{11}}\frac{e_{12}}{\beta\epsilon_{11}}\gamma+\frac{1}{\epsilon_{11}}\right)\right)\right]\end{aligned} \tag{27}$$

where σ_{rr}, $\sigma_{\theta\theta}$ and σ_{zz} are radial, circumferential and azimuthal stress components, respectively.

Seven sets of boundary conditions, henceforth referred to as cases 1, 2, 3, 4, 5, 6 and 7, are examined. In case 1, the sphere is subjected to an internal uniform pressure, zero electric potential difference across the spherical annulus, and free mechanical boundary conditions on the outer surface. In this case, the sphere acts as a sensor.

In the 2nd case, free mechanical boundary conditions on both internal and external surfaces were imposed. However, there is a uniform potential difference prescribed across the annulus. In this case, the sphere acts as an actuator. For convenience, it is assumed that outer surface potential is zero, and the potential on the inner surface is a nonzero constant. Case 3 is a combined loading case, i.e. a superposition of cases 1 and 2. In case 4, the sphere is subjected to an external uniform pressure, zero electric potential difference across the spherical annulus, and free mechanical boundary conditions on the inner surface. Case 5 is the combined loading case, i.e. a superposition of cases 1 and 4. In case 6 the sphere is subjected to an external uniform pressure and a uniform potential difference between the inner and outer surfaces of the sphere. Case 6 is a superposition of cases 2 and 4. Case 7 is also a combined loading, i.e. a superposition of the first and the sixth cases. In this case the sphere is subjected to uniform pressures on the inner and outer surfaces of the sphere and a certain voltage difference between these surfaces. The boundary conditions for each case can be written as follow:

Case 1:
$$\sigma_{rr}(1)=-P_i,\ \sigma_{rr}(\eta)=0,\ \phi_1(1)=0,\ \phi_1(\eta)=0 \tag{28}$$

Case 2:
$$\sigma_{rr}(1)=0,\ \sigma_{rr}(\eta)=0,\ \phi_1(1)=\phi,\ \phi_1(\eta)=0 \tag{29}$$

Case 3:
$$\sigma_{rr}(1)=-P_i,\ \sigma_{rr}(\eta)=0,\ \phi_1(1)=0,\ \phi_1(\eta)=0 \tag{30}$$

Case 4:
$$\sigma_{rr}(1)=0,\ \sigma_{rr}(\eta)=-P_o,\ \phi_1(1)=0,\ \phi_1(\eta)=0 \tag{31}$$

Case 5:
$$\sigma_{rr}(1)=-P_i,\ \sigma_{rr}(\eta)=-P_o,\ \phi_1(1)=0,\ \phi_1(\eta)=0 \tag{32}$$

Case 6:
$$\sigma_{rr}(1)=0,\ \sigma_{rr}(\eta)=-P_o,\ \phi_1(1)=\phi,\ \phi_1(\eta)=0 \tag{33}$$

Case 7:
$$\sigma_{rr}(1)=-P_i,\ \sigma_{rr}(\eta)=-P_o,\ \phi_1(1)=\phi,\ \phi_1(\eta)=0 \tag{34}$$

where the constants, P_i, P_o and ϕ are the prescribed dimensionless internal pressure, external pressure and potential, respectively and η is aspect ratio, i.e. $(\eta=b/a)$. For simplicity the boundary conditions are normalized as: $P_i=1, P_o=1$ and $\phi=1$, therefore the boundary conditions (28) ~ (34) can be written as:

Case 1:
$$\sigma_{rr}(1)=-1,\ \sigma_{rr}(\eta)=0,\ \phi_1(1)=0,\ \phi_1(\eta)=0 \quad (35)$$

Case 2:
$$\sigma_{rr}(1)=0,\ \sigma_{rr}(\eta)=0,\ \phi_1(1)=\phi,\ \phi_1(\eta)=0 \quad (36)$$

Case 3:
$$\sigma_{rr}(1)=-1_i,\ \sigma_{rr}(\eta)=0,\ \phi_1(1)=1,\ \phi_1(\eta)=0 \quad (37)$$

Case 4:
$$\sigma_{rr}(1)=0,\ \sigma_{rr}(\eta)=-1,\ \phi_1(1)=0,\ \phi_1(\eta)=0 \quad (38)$$

Case 5:
$$\sigma_{rr}(1)=-1,\ \sigma_{rr}(\eta)=-1,\ \phi_1(1)=0,\ \phi_1(\eta)=0 \quad (39)$$

Case 6:
$$\sigma_{rr}(1)=0,\ \sigma_{rr}(\eta)=-1,\ \phi_1(1)=1,\ \phi_1(\eta)=0 \quad (40)$$

Case 7:
$$\sigma_{rr}(1)=-1,\ \sigma_{rr}(\eta)=-1,\ \phi_1(1)=1,\ \phi_1(\eta)=0 \quad (41)$$

For each of the cases 1,2,3,4,5,6 and 7, the system of linear algebraic equations for the constants F_1, F_2, A_2 and A_2 can be written in the form

$$Ma_n=b_n \quad (n=1,\cdots,7) \quad (42)$$

where the 4×4 coefficient matrix M is defined in terms of column vectors:

$$M=\lceil m_1\ m_2\ m_3\ m_4\rfloor \quad (43)$$

where

$$m_1=\begin{bmatrix} \left(C_{11}\alpha_1+2C_{12}+\alpha_1 e_{11}\left(\frac{e_{11}}{\epsilon_{11}}+\frac{2}{\alpha_1}\frac{e_{12}}{\epsilon_{11}}\right)\right) \\ \left(C_{11}\alpha_1+2C_{12}+\alpha_1 e_{11}\left(\frac{e_{11}}{\epsilon_{11}}+\frac{2}{\alpha_1}\frac{e_{12}}{\epsilon_{11}}\right)\right)\eta^{(\alpha_1-1)} \\ \left(\frac{e_{11}}{\epsilon_{11}}+\frac{2}{\alpha_1}\frac{e_{12}}{\epsilon_{11}}\right) \\ \left(\frac{e_{11}}{\epsilon_{11}}+\frac{2}{\alpha_1}\frac{e_{12}}{\epsilon_{11}}\right)\eta^{\alpha_1} \end{bmatrix} \quad (44)$$

$$m_2=\begin{bmatrix} \left(C_{11}\alpha_2+2C_{12}+\alpha_2 e_{11}\left(\frac{e_{11}}{\epsilon_{11}}+\frac{2}{\alpha_2}\frac{e_{12}}{\epsilon_{11}}\right)\right) \\ \left(C_{11}\alpha_2+2C_{12}+\alpha_2 e_{11}\left(\frac{e_{11}}{\epsilon_{11}}+\frac{2}{\alpha_2}\frac{e_{12}}{\epsilon_{11}}\right)\right)\eta^{(\alpha_2-1)} \\ \left(\frac{e_{11}}{\epsilon_{11}}+\frac{2}{\alpha_2}\frac{e_{12}}{\epsilon_{11}}\right) \\ \left(\frac{e_{11}}{\epsilon_{11}}+\frac{2}{\alpha_2}\frac{e_{12}}{\epsilon_{11}}\right)\eta^{\alpha_2} \end{bmatrix} \quad (45)$$

$$m_3=\begin{bmatrix} \left[\frac{1}{r^2}\left((2C_{12}-C_{11})\frac{e_{12}}{\beta\gamma\epsilon_{11}}-e_{11}\left(-\frac{2e_{12}}{\epsilon_{11}}\frac{e_{12}}{\beta\gamma\epsilon_{11}}+\frac{e_{11}}{\epsilon_{11}}\frac{e_{12}}{\beta\epsilon_{11}}\gamma+\frac{1}{\epsilon_{11}}\right)\right)\right] \\ \left[\frac{1}{r^2}\left((2C_{12}-C_{11})\frac{e_{12}}{\beta\gamma\epsilon_{11}}-e_{11}\left(-\frac{2e_{12}}{\epsilon_{11}}\frac{e_{12}}{\beta\gamma\epsilon_{11}}+\frac{e_{11}}{\epsilon_{11}}\frac{e_{12}}{\beta\epsilon_{11}}\gamma+\frac{1}{\epsilon_{11}}\right)\right)\right]\frac{1}{\eta^2} \\ \left(-\frac{2e_{12}}{\epsilon_{11}}\frac{e_{12}}{\beta\gamma\epsilon_{11}}+\frac{e_{11}}{\epsilon_{11}}\frac{e_{12}}{\beta\epsilon_{11}}\gamma+\frac{1}{\epsilon_{11}}\right) \\ \left(-\frac{2e_{12}}{\epsilon_{11}}\frac{e_{12}}{\beta\gamma\epsilon_{11}}+\frac{e_{11}}{\epsilon_{11}}\frac{e_{12}}{\beta\epsilon_{11}}\gamma+\frac{1}{\epsilon_{11}}\right)\frac{1}{\eta} \end{bmatrix} \quad (46)$$

$$m_4=\begin{bmatrix}0\\0\\1\\1\end{bmatrix} \quad (47)$$

Each set of boundary conditions determines the form of the column vector b on the right hand side of equation (42). Thus $b_1, b_2, b_3, b_4, b_5, b_6$ and b_7 correspond to cases 1,2,3,4,5,6 and 7, respec-

tively:

$$b_2=\begin{bmatrix}0\\0\\1\\0\end{bmatrix},\ b_3=\begin{bmatrix}-1\\0\\1\\0\end{bmatrix},\ b_4=\begin{bmatrix}0\\-1\\0\\0\end{bmatrix},\ b_5=\begin{bmatrix}-1\\-1\\0\\0\end{bmatrix},\ b_6=\begin{bmatrix}0\\-1\\1\\0\end{bmatrix},\ b_7=\begin{bmatrix}-1\\-1\\1\\0\end{bmatrix} \tag{48}$$

Since $Ma_n=b_n$ $(n=1,\cdots,7)$, where

$$a_n=\begin{bmatrix}F_{1n}\\F_{2n}\\A_{1n}\\A_{2n}\end{bmatrix} \tag{49}$$

the unknown constants F_1, F_2, A_1 and A_2 for two piezoceramics, tabulated in Tables 1 and 2 have been obtained by the Cramer's rule, and accordingly:

$$F_{1n}=\frac{|M_{1n}|}{|M|},\ F_{2n}=\frac{|M_{2n}|}{M},\ A_{1n}=\frac{|M_{3n}|}{|M|},\ A_{2n}=\frac{|M_{4n}|}{|M|} \tag{50}$$

where

$$M_{1n}=[b_n\ m_2\ m_3\ m_4]$$
$$M_{2n}=[m_1\ b_n\ m_3\ m_4] \tag{51}$$
$$M_{3n}=[m_1\ m_2\ b_n\ m_4]$$

4. Results for the Piezoceramics PZT_5 and (Pb) (CoW) TiO_3

The numerical results are drawn in diagrams showing the variation of stress and potential across the thickness of the sphere. The piezoelectric materials PZT_5 and (Pb) (CoW) TiO_3 have been selected because of their technological importance. Mechanical and electrical properties of

Table 1 Constant values F_1, F_2, A_1 and A_2 for PZT-5 determined from seven sets of boundary conditions

	η	F_1	F_2	A_1	A_2
Case 1:	1.3	0.0595	−0.6383	−1.8006e+3	−3.3401
	2	0.0127	−0.3382	−830.9517	−1.0023
	4	−6.3903e−7	−0.2501	−553.7986	−0.3341
Case 2:	1.3	0.0632	−0.6387	−1.8006e+03	−3.3402
	2	0.0163	−0.3387	−830.9664	−1.0023
	4	0.0035	−0.2510	−553.8256	−0.3342
Case 3:	1.3	0.0661	−0.6156	−1.8004e+03	−3.3400
	2	0.0168	−0.3242	−830.8550	−1.0022
	4	0.0035	−0.2380	−553.7423	−0.3341
Case 4:	1.3	−0.0035	−0.0121	−0.0563	2.4846e−005
	2	−0.0041	−0.0140	−0.0967	−4.7063e−05
	4	−0.0066	−0.0227	−0.1972	−1.7374e−04
Case 5:	1.3	−0.0037	3.2221e−004	0.0099	3.1918e−005
	2	−0.0036	5.3092e−004	0.0147	4.0791e−005
	4	−0.0035	9.3583e−004	0.0270	6.5070e−005
Case 6:	1.3	0.0565	−0.6614	−1.8008e+03	−3.3404
	2	0.0122	−0.3527	−831.0630	−1.0024
	4	−5.1262e−05	−0.2631	−553.8819	−0.3342
Case 7:	1.3	0.0595	−0.6383	−1.8006e+03	−3.3401
	2	0.0127	−0.3382	−830.9517	−1.0023
	4	−6.3903e−07	−0.2501	−553.7986	−0.3341

Table 2 Constant values F_1, F_2, A_1 and A_2 for (Pb) (CoW) TiO_3 determined from seven sets of boundary conditions

	η	F_1	F_2	A_1	A_2
Case 1 :	1.3	0.0409	−0.1327	113.9464	−3.3427
	2	0.0070	−0.0705	52.5701	−1.0026
	4	−0.0017	−0.0518	35.0124	−0.3332
Case 2 :	1.3	0.0453	−0.1330	113.9565	−3.3433
	2	0.0114	−0.0710	52.5853	−1.0034
	4	0.0023	−0.0526	35.0419	−0.3345
Case 3 :	1.3	0.0489	−0.1247	113.9504	−3.3435
	2	0.0119	−0.0656	52.5800	−1.0034
	4	0.0023	−0.0478	35.0369	−0.3345
Case 4 :	1.3	−0.0080	−0.0080	−0.0040	8.5485e−004
	2	−0.0049	−0.0049	−0.0099	8.0300e−004
	4	−0.0040	−0.0040	−0.0245	0.0013
Case 5 :	1.3	−0.0045	2.9394e−004	−0.0100	6.1672e−004
	2	−0.0043	4.8608e−004	−0.0152	7.9882e−004
	4	−0.0040	8.5077e−004	−0.0295	0.0013
Case 6 :	1.3	0.0373	−0.1410	113.9525	−3.3424
	2	−0.0759	−0.0759	52.5755	−1.0026
	4	−0.0017	−0.0566	35.0174	−0.3333
Case 7 :	1.3	0.0409	−0.1327	113.9464	−3.3427
	2	0.0070	−0.0705	52.5701	−1.0026
	4	−0.0017	−0.0518	35.0124	−0.3332

Table 3 Material properties for piezoelectric materials

Property	PZT_	(Pb) (CoW) TiO_3
C_{11} (all GPa)	111.0	128.0
C_{22}	120.0	150.0
C_{33}	120.0	150.0
C_{44}	22.6	56.5
C_{55}	21.1	55.2
C_{66}	21.1	55.2
C_{12}	75.1	32.3
C_{13}	75.1	32.3
C_{23}	75.2	37.1
e_{11} (C/m^2)	15.78	8.5
e_{12} (C/m^2)	−5.35	1.61
ϵ_{11}/ϵ_0	1700	209
ϵ_{33}/ϵ_0	1730	238

piezoelectric materials are tabulated in Table 3 (Heyliger and Wu, 1998). The plots in the figures depict results for each of the seven boundary conditions (35) ~ (41), with three different aspect ratios, $\eta=1.3, 2$ and 4. All quantities are plotted versus dimensionless radius $\rho=r/a$. Since $1\leq\rho\leq\eta$, the plot for a given aspect ratio will terminate at respective value of η. In Figs. 2-7, the piezoceramic PZT_5, is shown by solid line and the piezoceramic (Pb) (CoW) TiO_3, by dashed line.

In Fig. 2, results are shown for case 1, where internal pressure is applied. The compressive radial stress, shown in Fig. 2(a), increases monotonically from its prescribed values of −1, at the inner radius, to 0, at the outer radius. In Fig. 2 (b), the tensile hoop stress is monotonically decreased from the inner to the outer radius. Its magnitude decreases with increasing aspect ratio, and its value at the outer radius approaches zero

for large aspect ratios. Although the boundary conditions for case 1 require that the potential be zero at inner and outer radii, Fig. 2(c) shows the resulting induced electrical effect, and an electric potential has developed through thickness of the sphere. As the aspect ratio increases, the location of minimum potential tends to move towards the inner radius. In this figure, the piezoceramic

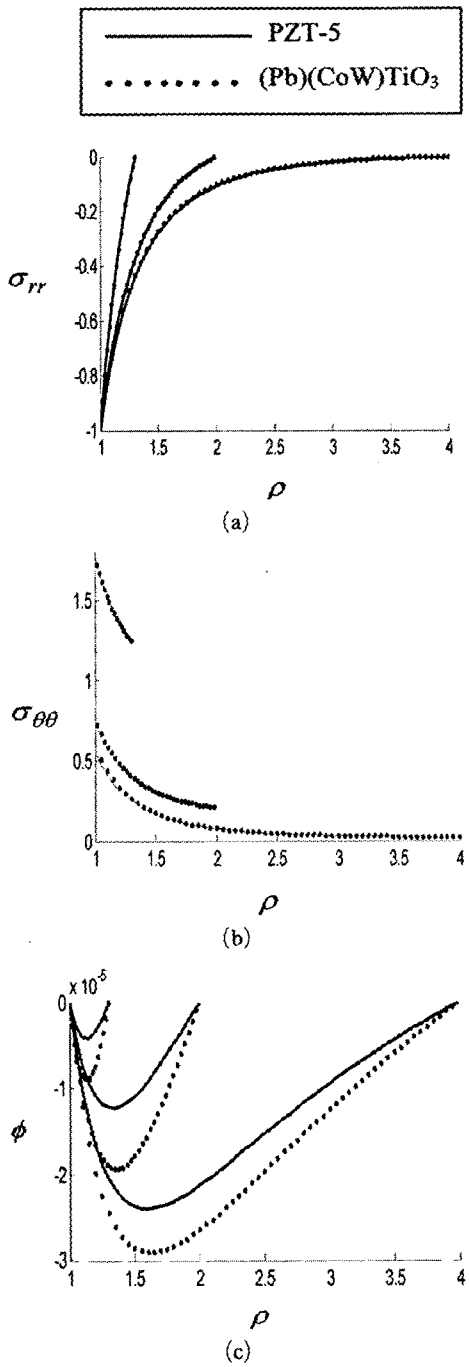

Fig. 2 Case 1: Plots for stresses and potential for $\eta=1.3,2,4\ (\eta=b/a)$

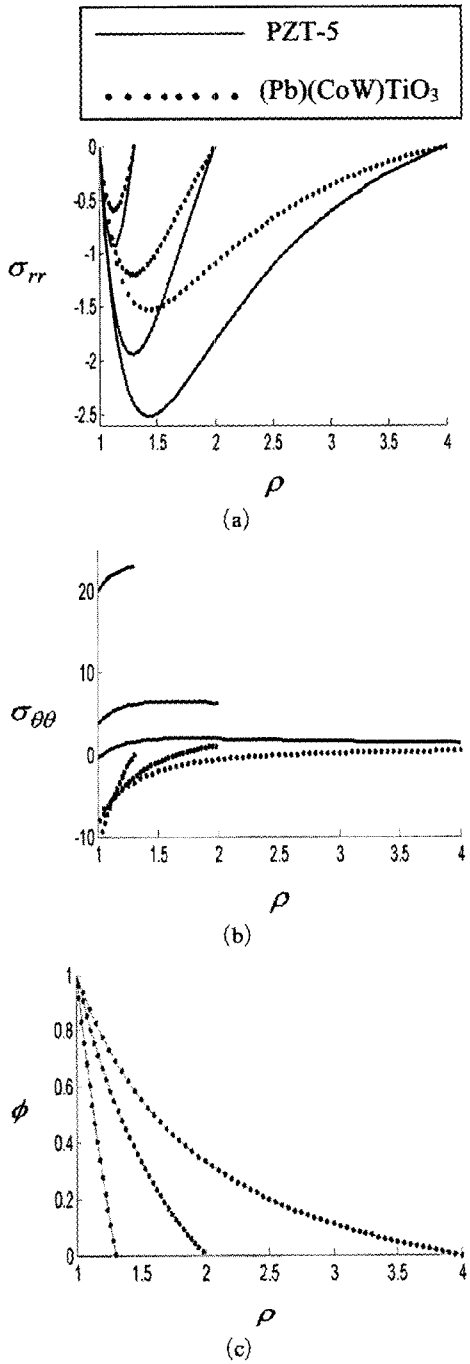

Fig. 3 Case 2: Plots for stresses and potential for $\eta=1.3,2,4\ (\eta=b/a)$

(Pb) (CoW) TiO_3 for each aspect ratio develops a greater electric potential than PZT-5.

Figure 3 shows the results of case 2 (purely electrical) boundary conditions. The compressive radial stresses plotted in Fig. 3(a) are interestingly minimum in the interior surface. For an aspect ratio of 1.3, the minimum radial stress is almost in the middle of the sphere thickness. As the aspect ratio η, increases to 4, the minimum radial stress shifts to the inner radius. In Fig. 3 (b), the hoop stress is monotonically increased from the inner to the outer radius. Its magnitude increases with increasing aspect ratio, and approaches to a constant value for larger aspect ratios. In Fig. 3(c), the electric potential at the inner surface has been fixed to 1, whereas the outer sphere surface is found to have zero potential.

Case 3 (Fig. 4) is a superposition of cases 1 and 2. The radial stress curves shown in Fig. 4(a) have minimum interior amount. For an aspect ratio of 1.3, the internal minimum stress is close to the middle of the sphere thickness. As η increases to 4, the location of minimum radial stress shifts far to the left, resulting a change in the curvature from concave up to concave down on the far right side of the plot. For each aspect ratio, the radial stress at the inner surface has been fixed to -1, whereas the outer surface of the sphere is set to zero. In this figure, the piezoceramic (Pb) (CoW) TiO_3 for each aspect ratio develops a greater radial stresses than PZT-5. Hoop stress plots shown in Fig. 4(b) have similar shapes to those in Fig. 3(b) (case 2). The electric potentials are shown in Fig. 4(c). For $\eta=1.3$ and $\eta=2$, the potentials decrease almost linearly from the proposed value of 1 at the inner radius to zero at the outer radius. Careful examination reveals that $\eta=2$ potential curve is slightly concave up. This trend is more apparent in the $\eta=4$ graph, where the potential has the concavity already seen in Fig. 3.

In Fig. 5, results are shown for case 4, where external pressure is applied. The compressive radial stress curve in case 4 boundary conditions decreases monotonically from proposed value of zero at the inner radius to -1 at the outer radius Fig. 5(a). The compressive hoop stress shown in Fig. 5(b) decreases from the inner to the outer radius. The magnitude decreases with increasing aspect ratio, and values at the outer radius

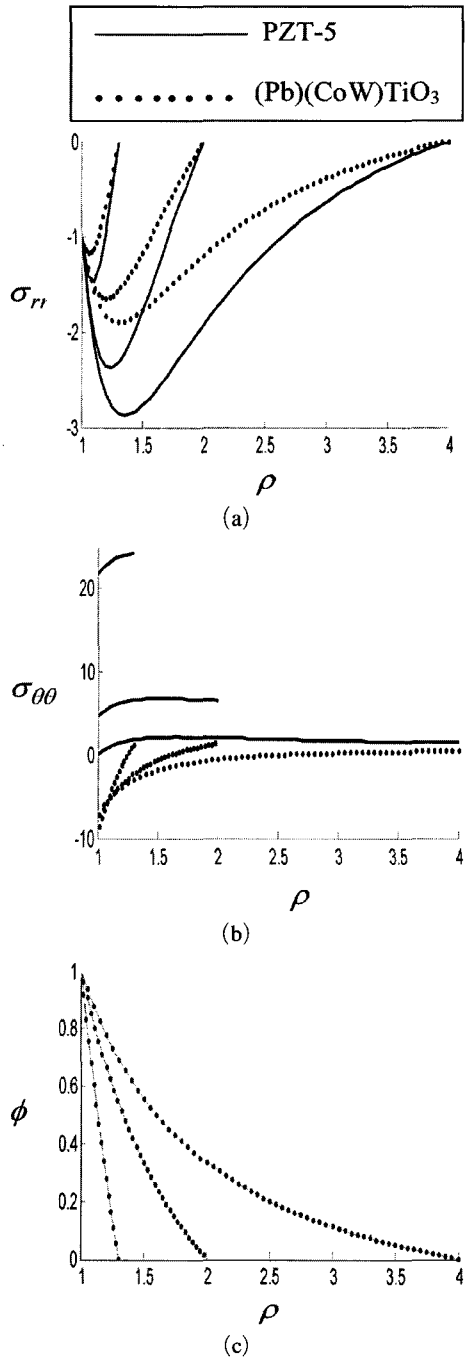

Fig. 4 Case 3: Plots for stresses and potential for $\eta=1.3,2,4$ ($\eta=b/a$)

approaches zero for larger aspect ratios. Interestingly the curves of two materials intersect. That is, (Pb) (CoW) TiO_3, (dashed line) exhibits a slightly lower value of hoop stress near the inner radius than PZT-5, but a higher value of hoop stress near the outer radius. Fig. 5(c) shows the induced electrical effect. Although the boundary conditions for case 4 require that the electrical

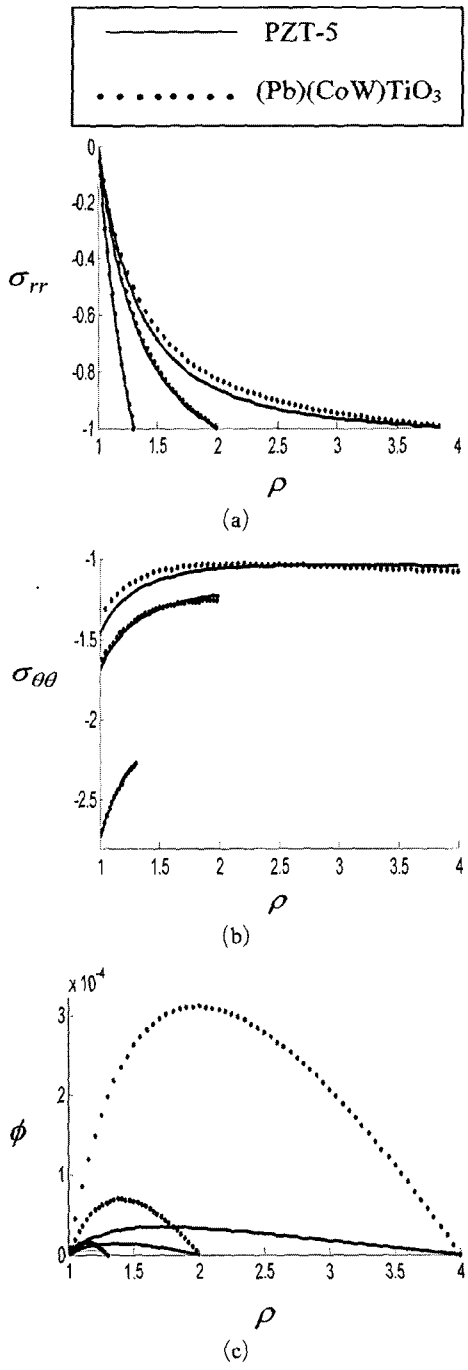

Fig. 5 Case 4: Plots for stresses and potential for $\eta=1.3,2,4$ ($\eta=b/a$)

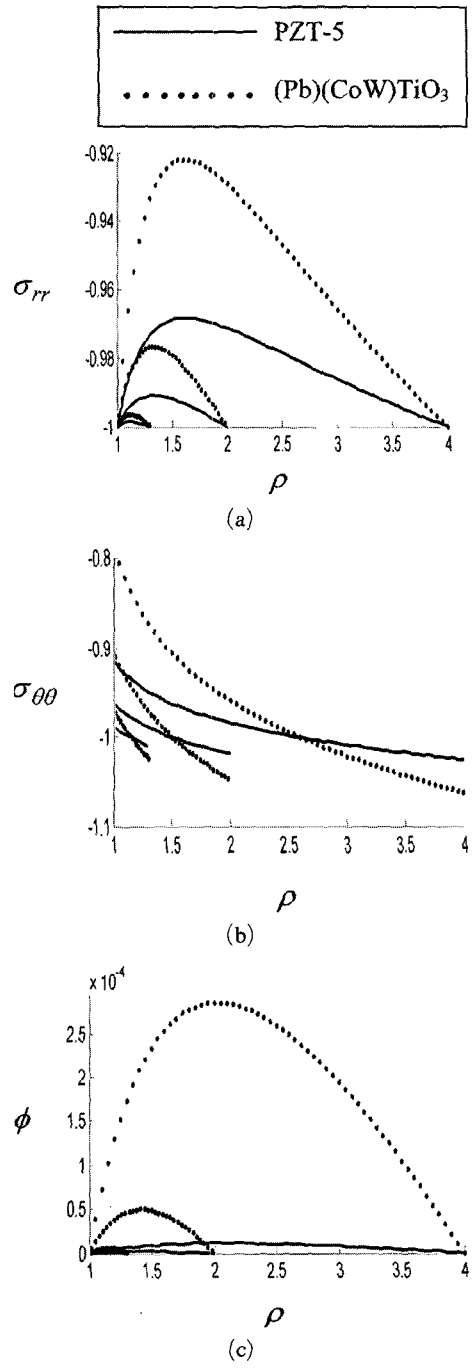

Fig. 6 Case 5: Plots for stresses and potential for $\eta=1.3,2,4$ ($\eta=b/a$)

potential be zero at the inner and outer radii, an electric potential has developed in the interior of the thickness. The location of the maximum potential tends to move towards the inner radius. The piezoelectric (Pb)(CoW)TiO_3 develops a greater electric potential than PZT-5.

The results of case 5, where internal and external pressures are applied, are shown in Fig. 6.

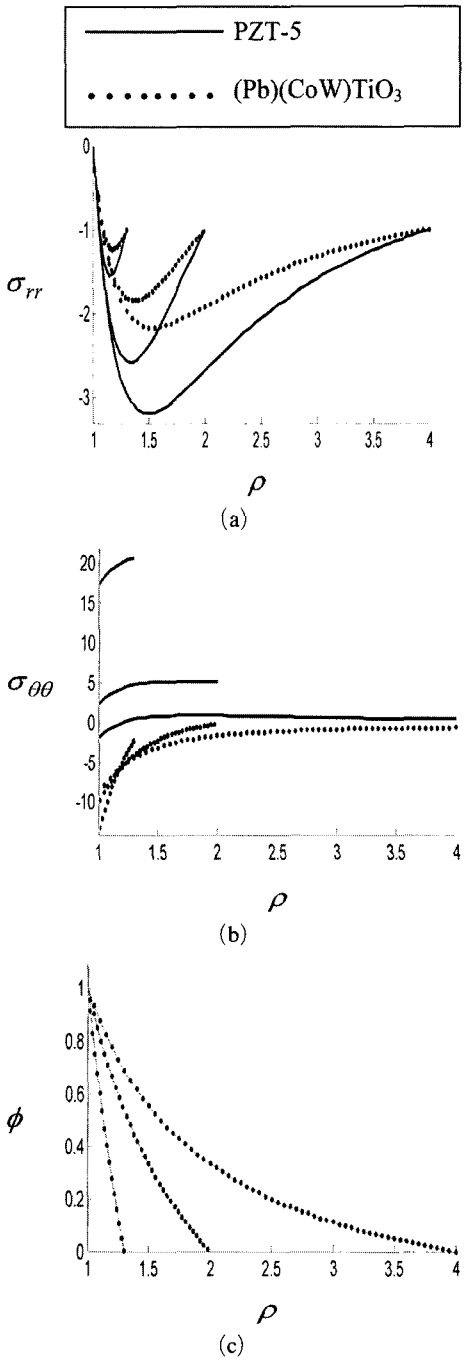

Fig. 7 Case 6: Plots for stresses and potential for $\eta=1.3,2,4$ ($\eta=b/a$)

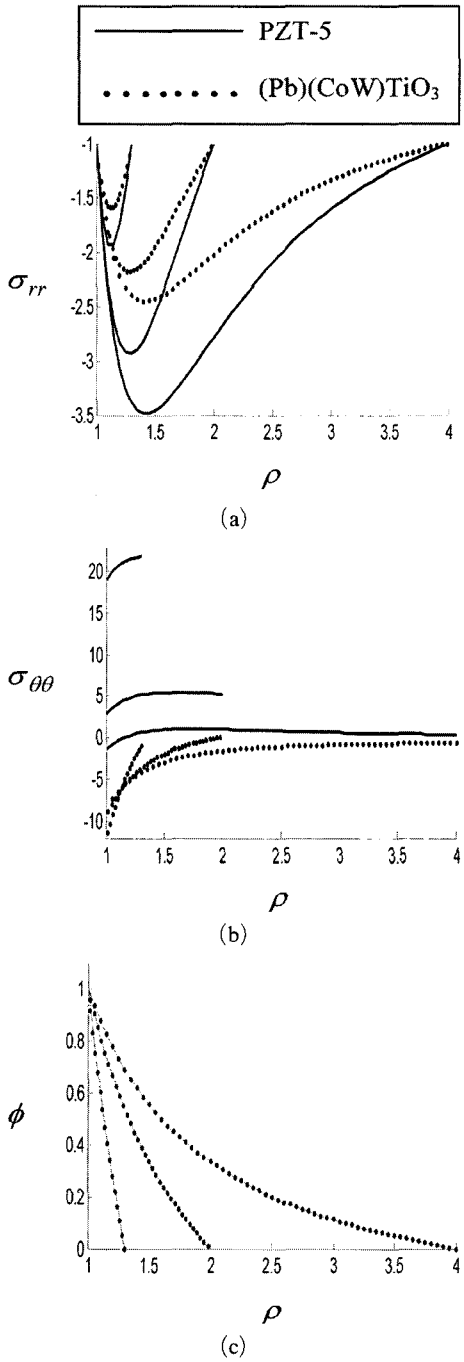

Fig. 8 Case 7: Plots for stresses and potential for $\eta=1.3,2,4$ ($\eta=b/a$)

The compressive radial stress shown in Fig. 6(a), has developed across the thickness of sphere. As the aspect ratio increases, the location of the maximum compressive radial stress tends to move towards the inner radius. The piezoceramic PZT-5 develops a greater compressive radial stress than (Pb) (CoW) TiO_3 for each aspect ratio. Hoop stress plots for case 5 boundary conditions are shown in Fig. 6(b). The graphs of each aspect ratio for both piezoceramics are monotonically decreasing. Same as case 4 the graphs of the two materials intersect and the piezoceramic (Pb) (CoW) TiO_3 develops a lower value of hoop stress near the inner radius than PZT-5, but a higher value of hoop stress near the outer radius. Fig. 6(c) shows the induced electrical effect. Although the boundary conditions for case 5 require that the electric potential be zero at the inner and the outer radii, an electric potential has been developed across the thickness of sphere. As aspect ratio increases, the location of the maximum potential tends to approach the inner radius. For $\eta=4$, the piezoceramic (Pb) (CoW) TiO_3 develops a greater electric potential than PZT-5. For $\eta=1.3$ and $\eta=2$, the electric potential for the two materials are similar.

Case 6, Fig. 7, is a superposition of cases 4 and 2, leading to the superposition of Figs. 3 and 5.

Figure 8 results from case 7, i.e. superposition of cases 1 and 6, and Figs. 2 and 7 accordingly.

Radial stresses, hoop stresses and electric potential in Fig. 7 (case 6) and Fig. 8 (case 7) have similar shapes to those in Fig. 3 (case 2).

5. Conclusions

In this research the static behavior of radially polarized piezoelectric hollow spheres was studied and the following results were concluded:

(1) In geometrically symmetric shapes, e.g. a piezoelectric sphere that can be polarized in radial direction, mechanical and electrical effects can be investigated separately. The analysis approach presented in this research can be applied on all radially polarized piezoelectric spheres.

(2) A solution to the problem of static radial displacement and potential field of a piezoelectric spherically isotropic hollow sphere, polarized in the radial direction for seven different sets of boundary conditions was obtained.

(3) Dimensionless stress distributions and electric potential curves were drawn and discussed in detail for two piezoceramics, namely PZT_5 and (Pb) (CoW) TiO_3 which have various applications in industry.

(4) The hoop stress comparing to the radial stress causes failure of the elastic hollow spheres. For two piezoceramics, at the first loading case in which a sphere is subjected to just uniform internal pressure (Fig. 2), hoop stress distribution on internal surface of the sphere is tensile for each aspect ratio which provides an appropriate location for fatigue crack growth.

(5) The technological implications of this study are significant, e.g. the amount of hoop stress resulting from mechanical loads in a hollow piezoelectric sphere can be reduced or neutralized by a suitably applied electrical field.

References

Berlincourt, D. A., 1971, "Piezoelectric Crystals and Ceramics," *In: O. E. Mattiat (ed.)*, Ultrasonic Transducer Materials, Plenum Press, New York 63~124.

Chen, W. Q. and Shioya, T., 2001. "Piezothermoelastic Behavior of a Pyroelectric Spherical Shell," *J. Thermall Stress*, 24, pp. 105~120

Chen, W. Q., 1998, "Problems of Radially Polarized Piezoelastic Bodies," *International Journal of Solids and Structures* 36, pp. 4317~4332.

Destuynder, P., 1999, "A Few Remarks on the Controllability of an Aeroacoustic Model Using Piezo-Devices," *In: J. Holnicki-Szulc and J. Rodellar (eds)*, Smart Structures. Kluwer Academic Publishers, Dordrecht pp. 53~62.

Fung, Y. C. 1965. *Foundations of Solid Mechanics*, Prentice-Hall, New York.

Heyliger, P. and Wu, Y.-C., 1999. "Electroelastic Fields in Layered Piezoelectric Spheres," *International Journal of Engineering Science* 37, pp. 143~161.

Jiang, H. W., Schmid, F., Brand, W. and Tomlinson,

G. R., 1999, "Controlling Pantograph Dynamics Using Smart Technology," *In : J. Holnicki-Szulc and J. Rodellar (eds)*, Smart Kluwer structures. Academic Publishers, Dordrecht pp. 125~132.

Kawiecki, G., 1999, "Piezogenerated Elastic Waves for Structural Health Monitoring," *In : J. Holnicki-Szulc and J. Rodellar (eds)*, Smart Structures, Kluwer Academic Publishers, Dordrecht pp. 133~142.

Lekhnitskii, S. G., 1981, *Theory of Elasticity of an Anisotropic Body*, Mir Publishers, Moscow.

Love, A. E. H., 1927, *A Treatise on the Mathematical Theory of Elasticity*, Cambridge University Press, Cambridge.

Sinha, D. K., 1962. "Note on the Radial Deformation of a Piezoelectric, Polarized Spherical shell with a Symmetrical Distribution," *J. Acoust. Soc. Am.* 34, pp. 1073~1075.

Tiersten, H. F., 1969. *Linear Piezoelectric Plate Vibrations*, Plenum Press, New York.